Respiratory metabolism of illuminated leaves depends on CO2 and O2 conditions.

Guillaume Tcherkez, Richard Bligny, Elizabeth Gout, Aline Mahé, Michael Hodges, Gabriel Cornic

This manuscript has been published in PNAS (*Proceedings of the National Academy of Sciences USA*) Vol.105(2): 797-802 (2008)

Classification: Biological sciences/Plant biology

Respiratory metabolism of illuminated leaves depends on CO_2- and O_2-conditions

Guillaume Tcherkez[1,2,*], Richard Bligny[3], Elizabeth Gout[3], Aline Mahé[4], Michael Hodges[4] & Gabriel Cornic[2].

1. Plateforme Métabolisme-Métabolome IFR87, Bâtiment 630, Université Paris-Sud XI, 91405 Orsay cedex, France.
2. Département d'Ecophysiologie Végétale, Laboratoire Ecologie Systématique Evolution, CNRS UMR8079, Batiment 362, Université Paris-Sud XI, 91405 Orsay cedex, France.
3. Laboratoire de Physiologie Cellulaire Végétale, CNRS UMR5168, CEA-Grenoble, 17, rue des Martyrs, 38054 Grenoble cedex 09, France.
4. Institut de Biotechnologie des Plantes, CNRS UMR8618, Bâtiment 630, Université Paris-Sud XI, 91405 Orsay cedex, France.
* Corresponding author.

Corresponding author:

Dr Guillaume Tcherkez

Postmail address:
Département d'Ecophysiologie Végétale
ESE CNRS UMR8079
Batiment 362
Université Paris-Sud XI
91405 Orsay cedex, France.
E-mail: guillaume.tcherkez@u-psud.fr
Fax: +33 1 69 15 72 38

Manuscript information:

Total number of text pages: 21
Number of figures: 5
Number of tables: 3 (Supporting Information)
Number of words/characters (all included except Supporting Information): **6,227/39,838**

Abbreviations: DHAP, dihydroxyacetone phosphate; Fd-GOGAT, ferredoxin-dependent glutamine-2-oxoglutarate aminotransferase; Fum, fumarate; Mal, malate; NMR, nuclear magnetic resonance; PDH, pyruvate dehydrogenase complex; PEPC, phospho*enol*pyruvate carboxylase; Pyr, pyruvate; Succ, succinate; TCA, tricarboxylic acid.

Abstract

Day respiration is the process by which non-photorespiratory CO_2 is produced by illuminated leaves. The biological function of day respiratory metabolism is a major conundrum of plant photosynthesis research: since the rate of CO_2-evolution is partly inhibited in the light, it is viewed as either detrimental to plant carbon balance or necessary for photosynthesis operation (e.g. in providing cytoplasmic ATP for sucrose synthesis). Systematic variations in day respiration rate under contrasting environmental conditions have been used to elucidate the metabolic rationale of respiration in the light. Using isotopic techniques, we show that both glycolysis and the TCA cycle activities are inversely related to the ambient CO_2/O_2 ratio: day respiratory metabolism is enhanced under high photorespiratory (low-CO_2) conditions. Such a relationship also correlates with the DHAP/Glc-6-P ratio, suggesting that photosynthetic products exert a control on day respiration. Thus, day respiration is normally inhibited by phosphoryl (ATP/ADP) and reductive (NADH/NAD) poise, but up-regulated by photorespiration. Such an effect may be related to the need for NH_2-transfers during the recovery of photorespiratory cycle intermediates.

Introduction

It is now seventy years since Krebs and Johnson proposed the mechanism by which pyruvic acid is oxidised to CO_2, and now called the 'Krebs cycle' or TCA cycle (1,2). While the basics of the metabolic reactions involved in leaf respiration are known, intense efforts are still currently devoted to elucidating the regulation of the TCA cycle (and, more generally, of day respiration) in illuminated leaves (for a recent review, see ref. 3).

Leaf day respiration (non-photorespiratory CO_2 evolution in the light) is an essential metabolic pathway that accompanies photosynthetic CO_2 assimilation and photorespiration. It is widely accepted that leaf respiration is partly inhibited in the light when compared to darkness (4). This acceptance is based on several strong lines of evidence, ranging from gas-exchange to molecular studies (for a review, see ref. 4): *(i)* the inhibition is thought to cause the light-enhanced dark respiration (5); *(ii)* the pyruvate dehydrogenase (PDH) is down-regulated in the light (6,7); *(iii)* the metabolic flux through the TCA cycle in the light is reduced in both extracted mitochondria (8) and intact leaves (9,10); *(iv)* mitochondria experience high ATP/ADP and NADH/NAD^+ ratios in the light that inhibit NAD-dependent isocitrate dehydrogenase (11); and *(v)* carbohydrate molecules such as sucrose and glucose are prevented from entering glycolysis (9), due to a modification of phosphofructokinase activity by the allosteric effector Fru-2,6-bisphosphate (12). Nevertheless, not all leaf cells are photosynthetic (e.g. most epidermal cells, phloem and xylem) so that some 'heterotrophic' background respiration in the light is expected, but its contribution is minor.

Although inhibited by light, day respiration is critical for plant growth and leaf N assimilation, as it provides ATP for Suc synthesis and TCA cycle intermediates (e.g. 2-oxoglutarate and oxaloacetate) for ammonium assimilation and amino-acid synthesis (13). Thus for many years, the down-regulation of day respiration and of the TCA-cycle in the light has been viewed as a perplexing phenomenon. It may be argued that the partial inhibition of

day respiration comes from a balance between two metabolic constraints: the energy requirement for Suc synthesis and the minimal competition between glycolysis and Suc synthesis for improved carbon gain. However, day respiration is additionally affected by other metabolic processes such as O_2 assimilation (photorespiration) (14), the rate of which depends on the internal CO_2/O_2 ratio. The photorespiratory cycle leads to Gly oxidative decarboxylation in the mitochondrion that supposedly gives rise to a large $NADH/NAD^+$ ratio, that in turn inhibits certain respiratory mitochondrial enzymes *in vivo* (11). Photorespiration is thus assumed to down-regulate day respiratory CO_2-evolution. Nevertheless, increased photorespiration rates could require more Glu cycling to provide amino groups for Gly synthesis in the peroxisomes. This higher demand might in turn require an increase in 2-oxoglutarate and Glu synthesis, and thus a higher day respiratory rate. The rationale of the metabolic homeostasis between day respiration and photorespiration are therefore currently uncertain.

To clarify the regulation of day respiration in illuminated leaves and its interactions with photorespiration, we have investigated the effect of the carboxylation-to-oxygenation ratio on day respiratory metabolic fluxes using isotopic $^{12}C/^{13}C$ spectrometry and ^{13}C and ^{31}P nuclear magnetic resonance (NMR). The results presented in this paper show that, while respiratory CO_2 evolution is always inhibited in the light when compared to the dark, the metabolic flux associated with the TCA cycle is inversely related to net CO_2 assimilation and this correlates with changes in phosphorylated metabolites levels. In addition, ^{13}C-distribution after labeling shows a larger commitment towards TCA intermediates and Glu as photorespiration increases. These findings, which are consistent with a role of day respiration in sustaining photorespiratory N cycling and perhaps nitrate assimilation, have important implications, ranging from the improvement of nitrogen use efficiency to the understanding of leaf and global ecosystem carbon budgets.

Results

In order to determine the amplitude and the steps of the leaf respiratory pathway that are inhibited in the light, detached leaves were fed with positionally labeled ^{13}C-enriched substrates (Pyr or Glc) and decarboxylation rates were measured by gas-exchange coupled to isotopic spectrometry. This method allowed us to calculate the decarboxylation rate in the light and, by comparing with the rate in darkness, the inhibition of decarboxylation in illuminated leaves. The positional labeling in Pyr allowed us to discriminate between the CO_2 produced by either the PDH (^{13}C-1-Pyr, ^{13}C-3-Glc) or the TCA cycle (^{13}C-2-Pyr, ^{13}C-1-Glc).

TCA-mediated decarboxylations are enhanced under low CO_2/O_2

When leaves were fed with ^{13}C-enriched Pyr, the apparent carbon isotope discrimination Δ_{obs} increased, showing that $^{13}CO_2$ was produced (Fig. 1A). Interestingly, the decarboxylation of ^{13}C-2-Pyr was low compared to that of ^{13}C-1-Pyr, showing the predominance of CO_2 produced by PDH as opposed to that produced by the TCA cycle. In addition, the smaller the CO_2/O_2 ratio, the larger the Δ_{obs} associated with ^{13}C-1-Pyr. A similar but modest trend occurred with ^{13}C-2-Pyr (Fig. 1A).

Dark-respired CO_2 was ^{13}C-enriched compared to the natural abundance ($\delta^{13}C$ of –22.1±0.5‰) with both ^{13}C-1- and ^{13}C-2-Pyr, indicating that decarboxylation of Pyr was substantial (Fig. 1B). The decarboxylation of ^{13}C-1-Pyr in the dark was larger after a light period at low CO_2 (140 μL L^{-1}) compared to a high CO_2. Both ^{13}C-1- and ^{13}C-2-Pyr were more decarboxylated in the dark after leaves had been exposed to light under low-O_2 conditions (Fig. 1B), and this was sensitive to O_2-conditions in the dark.

The isotopic data shown in Figure 1 were used to calculate the decarboxylation rates (Fig. 2) associated with PDH and the TCA cycle using mass-balance equations (see Materials

and Methods). While the decarboxylation rate associated with PDH was inhibited by only 30% in the light (Fig. 2), TCA cycle-mediated decarboxylations were much lower in the light than in the dark, with an inhibition of around 80% under typical atmospheric conditions (400 µL L^{-1} CO_2 in 21% O_2). The inhibition of the PDH-mediated decarboxylation was relatively constant under the CO_2 and O_2 conditions investigated. In contrast, TCA-mediated decarboxylations were much more sensitive to low CO_2 conditions, with 35% inhibition only at 140 µL L^{-1} CO_2 in 21% O_2 (Fig. 2C). It should be noted that while the inhibition value associated with the TCA cycle was similar in 400 µL L^{-1} CO_2 2% O_2 and in 400 µL L^{-1} CO_2 21% O_2, the absolute decarboxylation value was larger in 2% O_2 both in the dark and in the light (Fig. 2). This effect was due to a higher stomatal conductance in 2% O_2 and subsequently, larger transpiration rates that induced a higher absorption of labeled compounds (data not shown). Such a positive effect of low O_2 conditions on stomatal conductance has already been observed in *Xanthium strumarium* (15).

The commitment to glycolysis is enhanced under low CO_2/O_2

Similar experiments were carried out with ^{13}C-enriched Glc to determine whether the glycolytic carbon flow changes under varying CO_2/O_2 conditions. Under typical conditions (400 µL L^{-1} CO_2 in 21% O_2), leaves fed with ^{13}C-1-Glc or ^{13}C-3-Glc did not produce significant amounts of $^{13}CO_2$ in the light, as indicated by the very small deviation of the apparent carbon isotope discrimination Δ_{obs} (Table S1 of the Supporting Information). The same applied to high CO_2-to-O_2 conditions (1000 µL L^{-1} CO_2 in 21% O_2), with a Δ_{obs} value of 24.5±0.5‰. In contrast, the decarboxylation of ^{13}C-1-Glc and ^{13}C-3-Glc became apparent in the light under low CO_2 conditions (140 µL L^{-1} in 21% O_2), with Δ_{obs} values increasing up to 106.4±13.8‰ (with ^{13}C-3-Glc, Table S1). This indicated that ^{13}C-Glc could be oxidised in the light by glycolysis and that PDH and TCA activities were both at the origin of the respired

$^{13}CO_2$ from ^{13}C-Glc. It should be noted that this increase was not an artefact caused by the low CO_2 mole fraction in the chamber (making decarboxylated CO_2 proportionally larger), because the CO_2 mole fraction was taken into account in the mass-balance-based calculations. In darkness, the $\delta^{13}C$ value of respired CO_2 increased to 365‰ (with ^{13}C-3-Glc) after photosynthesis at 400 μL L^{-1} CO_2, and 719‰ (with ^{13}C-3-Glc) after photosynthesis at 140 μL L^{-1} CO_2 in 21% O_2 (Table S1). When these values were used to calculate decarboxylation values, it was found that both TCA- and PDH-mediated decarboxylations were inhibited by nearly 90% at 400 μL L^{-1} CO_2, and 60% at 140 μL L^{-1} CO_2 in the light (Table S2 of the Supporting Information). These data show that leaf CO_2 levels modulate the entry of Glc molecules into the glycolytic and respiratory pathways both in the light and the dark; Glc is a better respiratory substrate at low CO_2 levels.

Distribution of the ^{13}C-label in metabolites

To gain information on the changes in metabolic pathways under the different CO_2/O_2 conditions in the light, the fate of the ^{13}C-atoms (from ^{13}C-substrate feeding) was determined in leaf metabolites by ^{13}C-NMR analyses. Leaves were fed with positionally-enriched (99% ^{13}C) substrates under either 140, 400, or 1000 μL L^{-1} CO_2 in 21% O_2 and the positional isotopic abundances of identified metabolites (in % of ^{13}C), measured by NMR, are displayed as an isotopomics array (Fig. 3). As expected, hexoses and Glc- or Fru-moieties of Suc were ^{13}C-labeled when ^{13}C-Glc was supplied to leaves so that several C-1 and C-6 positions formed clusters (these positions are redistributed by aldolase and triose-phosphates isomerase reactions). The C-4 and C-5 positions in hexoses clustered near to the C-3 positions, indicating that a redistribution of ^{13}C label occurred in the light through the pentose-phosphate pathway.

The flux through the pentose-phosphate cycle may be estimated with both NMR and gas-exchange data. At 140 μL L^{-1} CO_2, the ^{13}C-amount in the C-atom positions redistributed by the pentose-phosphate cycle (i.e. the ^{13}C-amount in C-2, C-3, C-4 and C-5 after ^{13}C-1-Glc labeling and the ^{13}C-amount in C-1, C-2, C-5 and C-6 after ^{13}C-3-Glc labeling), as found by NMR after labeling, corresponds to a ^{13}C flux of 0.03 μmol m^{-2} s^{-1}. With the gas-exchange data, the flux through the pentose-phosphate cycle can be estimated by the excess of calculated CO_2 production from the TCA with respect to the PDH, because the pentose-phosphate cycle involves the decarboxylation of the C-1 atom of Glc. With ^{13}C-1-Glc labeling, The TCA-mediated decarboxylation rate was 0.11 μmol m^{-2} s^{-1} while the PDH-mediated decarboxylation was 0.07 μmol m^{-2} s^{-1} (Table S2 of the Supporting information). The CO_2 production by the pentose-phosphate cycle was thus of 0.04 μmol m^{-2} s^{-1}, a value that is very close to that obtained with NMR. Such a value is nevertheless not enough to explain the entire $^{13}CO_2$ production from ^{13}C-Glc at low CO_2, so that the enhancement of the commitment to glycolysis still holds under this condition.

The commitment to the TCA cycle can be assessed with ^{13}C-labeling in organic acids. Some organic- and amino-acids clustered on the upper part of Fig. 3, with positional ^{13}C-enrichment generally lower than 10%. However, the C-2 atom of malate and the C-2 and C-3 atoms of Glu were clearly labeled when ^{13}C-Pyr was supplied. This labeling was lower at high CO_2, and the same applied to the C-2 and C-3 atoms of fumarate. Since these C-atom positions in malate, Glu and fumarate can only be labeled by the interplay (redistribution) of the TCA cycle, this labeling trend is indicative of an increase in TCA cycle activity. This view agrees with the increase of the ^{13}C-abundance in Glu, succinate and fumarate from high to low CO_2/O_2 ratios as shown in Fig. 4 (where ^{13}C-abundances are relative to those found in malate in order to take into account variations in refixed decarboxylated $^{13}CO_2$ by phospho*enol*pyruvate carboxylase (PEPC) activity, as discussed below).

Nevertheless, the lower ^{13}C-abundance in organic acids under high CO_2 conditions may also partly be due to the diluting effect of assimilated ^{12}C-enriched carbon (inlet CO_2 has a $\delta^{13}C$ value near to –50‰). This effect is expected in malate and fumarate, which are two major metabolites accumulated by *Xanthium* leaves. There was indeed a significant and negative correlation between the isotopic enrichment in fumarate C-2/3 and malate C-2 and the quantity of these organic acids (Fig. 4, inset). However, the correlation was reversed in the case of Glu C-2 (Fig. 4, inset) while there was no correlation at all with other organic acids or amino-acids (data not shown). Therefore, we conclude that the lower ^{13}C-enrichment in organic- and amino-acids at high CO_2 conditions was not only caused by an isotopic dilution but also by the decrease of the commitment of ^{13}C-Pyr to the TCA cycle.

$^{13}CO_2$ refixation

While the trend of ^{13}C-labeling in TCA cycle intermediates is clear, the rate of decarboxylation of ^{13}C-enriched substrates in the light and the ^{13}C-labeling of different metabolites may have been adulterated by $^{13}CO_2$ refixation by either PEPC or Rubisco. Indeed, $^{13}CO_2$ fixation by PEPC occurred under each CO_2 condition investigated in the present study, as revealed by the ^{13}C-enrichment in the C-4 of malate when ^{13}C-1-Pyr or ^{13}C-2-Pyr was supplied to leaves. However, the C-2 and C-3 positions in malate were also clearly ^{13}C-enriched under low CO_2 conditions when fed with ^{13}C-2-Pyr (Fig. 3), and this observation is consistent with an increased TCA cycle activity.

Metabolites could have been also ^{13}C-labeled *via* photosynthetic $^{13}CO_2$ refixation. The labeling of hexoses and Suc in the C-3 position after Pyr feeding (refixation of $^{13}CO_2$ decarboxylated from ^{13}C-1-Pyr by Rubisco) did occur but the maximum positional ^{13}C-abundance in C-3 indicates that the proportion of refixed ^{13}C in the whole molecule was about 0.7% only. Refixation of respired CO_2 into starch was also assessed after gas-exchange and

on-line apparent Δ_{obs} measurements (Fig. 1): the carbon isotope composition ($\delta^{13}C$) of starch was between –36.5 (minimum value obtained at 1000 μL L^{-1} CO_2, with ^{13}C-1-Pyr feeding) and –12.7‰ (maximum value obtained at 140 μL L^{-1} CO_2 with ^{13}C-1-Pyr feeding), indicating that the proportion of starch containing refixed CO_2 was between 0 and 0.4% only (see Table S3 of the Supporting Information). Therefore, although Rubisco-mediated refixation of decarboxylated $^{13}CO_2$ did occur, it was always very low.

Correlations with phosphorylated metabolites

Phosphorylated metabolites, such as dihydroxyacetone phosphate (DHAP), are known to be important regulators of the primary carbon metabolism of plant leaves (12,16). Therefore, we measured the amounts of phosphorylated compounds by ^{31}P-NMR spectroscopy on the same samples used for the ^{13}C-labeling and ^{13}C-NMR analyses. There was a clear linear and positive correlation between the activity of the TCA cycle, as witnessed by gas-exchange (values from Fig. 2), and the DHAP-to-Glc-6-phosphate ratio (Fig. 5, dashed line). In contrast, there was no statistically significant correlation with the DHAP/Pi ratio although a positive trend was apparent (Fig. 5, dotted line).

Discussion

Based on data from gas-exchange analyses to enzymatic activities (6,7,8,9), it has become widely accepted that leaf day respiration (non photorespiratory CO_2 evolution in the light) is inhibited in the light (for a review, see 3). However, the rationale and the effect of environmental conditions on day respiration and its inhibition are uncertain and solving such an issue is critical to understand how leaves adapt carbon partitioning between export of photosynthates and respiration or N economy under varying natural conditions. CO_2 and O_2 levels are two parameters of fundamental importance because the leaf internal CO_2/O_2 ratio

changes when environmental conditions alter stomatal closure (e.g. drought). Here, we have developed isotopic methods to provide evidence that respiratory metabolism is up-regulated when the CO_2/O_2 ratio decreases, and we argue that day respiration is an exquisite example of metabolic compromise between feedback inhibition by NADH and ATP, and 2-oxoglutarate precursor requirement for N metabolism.

The regulation of the TCA cycle

While no major effect on PDH-decarboxylation was observed, the carbon flow through the TCA cycle increased under low CO_2/O_2 conditions, as evidenced by the larger decarboxylation rate of ^{13}C-2-Pyr, so that the inhibition by light of the TCA cycle was 40% at 140 µL L^{-1} CO_2 as compared to nearly 90% under typical conditions (400 µL L^{-1} CO_2, Figs.1 and 2). Furthermore, the ^{13}C-labeling of succinate, citrate and Glu, as revealed by NMR tracing after ^{13}C-2-Pyr feeding, increased as the CO_2 mole fraction decreased (Fig. 4). In this context, the observed labeling in malate (Fig. 3), that indicated the simultaneous increase in PEPC activity, comes as no surprise: this is in agreement with the anapleurotic role of this enzyme, that compensates for 2-oxoglutarate consumption (for Glu synthesis) by feeding the TCA cycling with oxaloacetate molecules (17). The whole picture is thus consistent with an increased commitment to the TCA cycle and Glu production under low CO_2 conditions.

The up-regulation of the TCA metabolism under low CO_2 stems from a larger glycolytic carbon input, as evidenced by the enhancement of ^{13}C-3-Glc decarboxylation (see the Result section and Table S1 and S2) and the slight ^{13}C-labeling in malate C-2 after ^{13}C-Glc feeding (Fig. 3). In addition, as a consequence of the lower photosynthetic CO_2 fixation rate, the DHAP/Glc-6-P ratio decreased with CO_2 mole fraction, and importantly, this ratio was strongly correlated with the inhibition of the TCA cycle (Fig. 5). The relative abundance of triose phosphates is already known to be a metabolic parameter that controls carbon entry

to glycolysis by the interplay of the effector Fru-2,6-bisphosphate (12), and promotes pyruvate kinase activity (18). It thus appears clear that it also controls the commitment of carbon molecules to the respiratory pathway. Uncertainty nevertheless remains about whether it acts indirectly on the TCA cycle (through the enhancement of glycolysis) or not.

Interactions with photorespiration

The higher carbon flow through the TCA cycle under low CO_2 may appear somewhat paradoxical as it has often been supposed that large photorespiratory rates inhibit mitochondrial respiratory enzymes (11,19), such as the NAD-dependent isocitrate dehydrogenase (11). Accordingly, Gly decarboxylase antisense lines of potato (*Solanum tuberosum*) have lower decarboxylation rates in the light (as revealed by ^{14}C-labeling experiments) and the ATP/ADP as well as the NADH/NAD^+ ratios are both higher than in the wild type (20). In addition, the predominance of NADH production by Gly oxidation over that by the TCA cycle has been shown using isolated mitochondria under ADP-limiting conditions (21). This might reduce the NAD^+ available for the mitochondrial dehydrogenase steps of the TCA cycle. Our results show that the inhibition of day respiration occurs whatever the CO_2/O_2 ratio and furthermore, there is a lower inhibition value under very low-O_2 conditions (400 μL L^{-1} CO_2, 2% O_2) as compared to high-CO_2 conditions (1000 μL L^{-1} CO_2, 21% O_2) (Fig. 2). This would be consistent with a much reduced mitochondrial redox poise caused by the non-physiological, very low oxygen mole fraction.

However, we show here that the inhibition of the TCA cycle is relaxed under low-CO_2 conditions in 21% O_2 (see above). Isocitrate production is probably not influenced by such photorespiratory conditions, as citrate synthase remains active because of the very large K_i(ATP) (5 mmol L^{-1}) and the absence of any NADH effect (22). As the mitochondrial NAD-dependent isocitrate dehydrogenase is believed to be inhibited in the light, we suggest that

isocitrate is processed by the cytosolic or mitochondrial NADP-dependent isocitrate dehydrogenase (23). This bypass would allow to sustain the necessary Glu flow under photorespiratory conditions.

Possible rationale

The regulation of the TCA cycle by the CO_2/O_2 conditions may be viewed as a side effect of the drop in the DHAP relative quantity on the commitment to glycolysis and therefore respiration (see above and Fig. 5). Unless there are other prevailing imperatives (such as the need of NADH to reduce photorespiration-derived hydroxypyruvate or H_2O_2), it also reflects an increased need for Glu to feed photorespiratory N-recycling when conditions shift to low CO_2 mole fractions, simply because the production of Gly from glycolate would require a higher Glu flow. Unsurprisingly then, the production of the Glu-precursor 2-oxoglutarate by the TCA cycle is enhanced. The argument that photorespiration is beneficial for Glu synthesis is in agreement with the positive correlation between photorespiration and leaf nitrate reduction (24,25). This scenario is also consistent with the results obtained in the cytoplasmic male sterile CMSII mutant of tobacco (affected in the mitochondrial respiratory complex I) in which the day respiratory rate is similar or even higher than that of the wild type while both photorespiration and N-metabolism (amino-acid synthesis) are enhanced (26,27).

Therefore, we argue that day respiratory homeostasis in leaves is likely to be the result of a compromise between two opposing forces: *(i)* an inhibition of respiration and glycolysis due to high mitochondrial NADH levels generated by photorespiration (Gly decarboxylation) and elevated ATP/ADP and DHAP levels generated by photosynthetic activity; *(ii)* a stimulation of the TCA cycle in order to adjust 2-oxoglutarate production to photorespiratory Glu demand. Such a compromise should be very dynamic, adjusting to changes in environmental conditions that modify stomatal closure, thereby altering leaf internal CO_2/O_2

balance. For example, water deficit, that leads to a low internal CO_2 mole fraction, presumably promotes day respiration and photorespiration. Therefore, in the summer months the quantitative significance of these metabolic changes should be evident in many C_3 crops and natural vegetation. However, it is probable that such a promoting effect may disappear on a long-term basis because of acclimation processes (28,29). Thus the extent to which the regulation of day respiration by CO_2 and O_2 conditions scale up to crop productivity and global carbon sequestration needs further experimental assessment.

Material and methods

Plant material

Cocklebur (*Xanthium strumarium* L., Asteraceae) plants were grown in the greenhouse from seed in 100 mL pots of potting mix and transferred to 3 L pots after two weeks. Minimum photosynthetic photon flux density during a 16-h photoperiod was kept at approximately 400 μmol m^{-2} s^{-1} by supplementary lighting. Temperature and vapor pressure deficit were maintained at approximately 25.5/18.5^{o}C and 1.4/1.2 kPa day/night, respectively. The carbon isotope composition ($\delta^{13}C$) of CO_2 in the greenhouse air was –9.5±0.3‰. The third or fourth leaves (from the apical bud) were used for all measurements.

Gas exchange measurements

a- Closed system (dark respiration)

The respiration chamber was placed in a closed system, which was directly coupled to an elemental analyser (EA) NA-1500 (Carlo-Erba, Milan) through a 15-mL loop, as described in (30). After decarboxylating the system, respired CO_2 was accumulated until it reached nearly 300 μL L^{-1}. The loop was then shunted and the gas inside the loop was introduced into the EA

with helium for gas chromatography. The connection valve between the EA and the isotope ratio mass spectrometer (VG Optima, Micromass, Villeurbanne, France) was opened when the CO_2 peak emerged from the EA.

b- Open system (photosynthesis and on-line carbon isotope discrimination)

The photosynthesis system has already been described in (9). Briefly, a purpose-built assimilation chamber was connected in parallel to the sample air hose of the LI-6400 (Li-Cor Inc., Lincoln, NE). Leaf temperature was controlled at 21°C with circulating water from a cooling water bath to the jacket of the leaf chamber, and was measured with a copper-constantan thermocouple plugged to the thermocouple sensor connector of the LI-6400 chamber/IRGA. Inlet air was adjusted to *ca*. 10 mmol mol^{-1} H_2O and passed through the chamber at a rate of 30 L h^{-1}, monitored by the LI-6400. Light (400 µmol m^{-2} s^{-1}) was supplied by a 500 W halogen lamp (Massive N. V., Kontich, Belgium). Inlet CO_2 was obtained from a gas cylinder (Alphagaz N48, Air Liquide, France) with a $\delta^{13}C$ of –50.2±0.2‰. The outlet air of the chamber was regularly shunted and was sent to the loop to measure its $^{12}C/^{13}C$ isotope composition and thus the on-line carbon isotopic discrimination (Δ_{obs}). The gas inside the loop was introduced into the EA for GC as described above. Δ_{obs} during photosynthesis was measured following the method described by ref. (31). Air with 2% oxygen was from a cylinder (Crystal gas mixture, Air Liquide, France). When light was turned off, the leaf was immediately removed from the open system and one half was frozen in liquid nitrogen. The other half (still attached to the peduncle) was placed in the closed system for dark respiration measurements (see above).

Starch extraction

The protocol for starch extraction was similar to that described in (30). The frozen leaf material was lyophilised and powdered. 50 mg of leaf powder was suspended with 1 mL of distilled water in an Eppendorf tube (Eppendorf Scientific, Hamburg, Germany). After centrifugation, the pellet was washed four times with 95% ethanol at room temperature and starch was extracted by HCl solubilization and precipitated with cold methanol. After lyophilisation, starch was transferred to tin capsules (Courtage Analyze Service, Mont Saint-Aignan, France) for isotope analysis.

NMR analyses

Leaves used for NMR spectroscopy were fed for 2 h at 21°C and 400 µmol m^{-2} s^{-1} with either water (control), ^{12}C-substrates or ^{13}C-substrates in a large plexiglass chamber (surface area 450 cm²) connected in parallel to the sample air hose of the LI-6400 (Li-Cor Inc., Lincoln, NE), allowing CO_2 mole fraction monitoring.

NMR measurements were carried out as described in (9) and (32) from perchloric acid extracts prepared from 5 g of frozen leaf material. Spectra were obtained using a Bruker spectrometer (AMX 400) equipped with a 10-mm multinuclear probe tuned at 161.9 and 100.6 MHz for ^{31}P- and ^{13}C-NMR, respectively. The assignment of ^{13}C resonance peaks was carried out according to (33). Identified compounds were quantified from the area of their resonance peaks using fully relaxed conditions for spectra acquisition (pulses at 20 s intervals). Peak intensities were normalized to a known amount of the reference compound (maleate for ^{13}C and methyl-phosphonate for ^{31}P) that was added to the sample (internal standard).

^{13}C-enriched molecules

The positional ^{13}C-labeled molecules (99% ^{13}C in the considered position) were purchased from Eurisotop (Saclay, France). Pyruvate was dissolved in distilled water and the pH was adjusted to 6.7 with NaOH. To obtain non-fully labeled solutions (Δ_{obs} experiments), the labeled compounds were mixed with industrial glucose ($\delta^{13}C = -9‰$) or pyruvate ($\delta^{13}C = -21‰$) from Sigma. The resulting overall composition of glucose and pyruvate solutions was checked to be 2500‰ and 1400‰, respectively. In each case, the final concentration was 0.015 mol L^{-1}. The solutions were fed to the leaves through the transpiration stream.

Calculations

The procedure used to calculate the decarboxylation rates of ^{13}C-enriched substrates in the light from apparent Δ_{obs} values has already been explained in detail (9). Briefly, the difference between apparent Δ_{obs} values obtained with and without substrate addition is considered to reflect the additional decarboxylation flux in the light. Using mass balance equations, it can be shown that the decarboxylation rate r_{day} has the following form:

$$r_{day} = \frac{d}{SV_M} \cdot \frac{c_o\lambda_o - c_e\lambda_e + (c_e - c_o)\lambda_{fixed}}{\lambda_s - \lambda_{fixed}}$$

where d is the flow, S leaf surface area, V_M the molar volume at air temperature, c_e and c_o are the CO_2 mole fractions in inlet and outlet air, respectively. λ values are ^{13}C percentages (using delta-values is not possible because of large ^{13}C-enrichments) in inlet CO_2 (subscript e), outlet CO_2 (subscript o), net fixed CO_2 (subscript *fixed*), and ^{13}C-enriched added substrate (subscript s). This equation holds for homogeneously labeled substrates; it is somewhat changed for

positional enrichments to take into account the different origin of decarboxylated CO_2. This occurs when glucose or pyruvate are added: the C-1 atom of pyruvate is decarboxylated by PDH while the C-2 and C-3 positions are decarboxylated by the Krebs cycle. Similarly, the C-3 and C-4 atom positions of glucose are decarboxylated by the PDH reaction, the other being decarboxylated by the Krebs cycle. Taking advantage of positionally ^{13}C-enriched substrates: ^{13}C-1-pyruvate would specifically enrich the CO_2 produced by PDH while ^{13}C-2-pyruvate would specifically enrich the CO_2 that comes from the Krebs cycle. The same applies to positional ^{13}C-enrichment in glucose. It should be noted that, in contrast to the argument of ref. (3), any isotopic dilution of the substrate is taken into account as the observed carbon isotope discrimination is always a net value that integrates the decarboxylation of natural (that is, not added) Pyr or Glc molecules, both before and after ^{13}C-substrate addition.

A similar procedure applies to dark-respired CO_2 measurements. In other words, CO_2 that is produced in darkness (^{13}C-percentage λ_{global}) after a light period with ^{13}C-enriched substrate feeding comes from respiratory oxidation of new photosynthates (the ^{13}C-percentage in the net fixed carbon is λ_{fixed}), photosynthates from the previous light period in the greenhouse (^{13}C-percentage $\lambda_{previous}$), and additional C coming from the ^{13}C-enriched substrate fed to the leaf (^{13}C percentage λ_s). The night-decarboxylation rate has the following form:

$$r_{night} = R_n \cdot \frac{\lambda_{global} - \lambda_p}{\lambda_s - \lambda_p}$$

where λ_p is a linear combination of $\lambda_{previous}$ and λ_{fixed}. It is equal to 0.6 $\lambda_{previous}$+ 0.4 λ_{fixed} after 2-3 h in the light under ordinary CO_2/O_2 conditions (during which 200-400 mmol C m^{-2} have been fixed), and 0.5 $\lambda_{previous}$ + 0.5 λ_{fixed} after 2-3 h in the light under high CO_2 conditions (during which 400-800 mmol C m^{-2} have been fixed) (34). It should be noted that possible variations in these coefficients do only introduce very slight errors in the estimate of the ^{13}C-enriched substrate decarboxylation r_{night}, because of the strong ^{13}C-enrichment of the

substrate (that is, the λ_p value is always very small compared to λ_{global} or λ_s and may be neglected). Again, that relationship is somewhat modified with positional enrichments to take into account the different origin of decarboxylated CO_2 (as described in 9).

Clustering analysis

The ^{13}C-NMR data were represented as an isotopomic array as described in (35). The positional isotopic abundances (in ^{13}C-percentage) relative to the natural ^{13}C-abundance (1.1%) are indicated by colors so that black cells indicate near-natural abundance, green and red cells indicate lower- and larger-than-natural ^{13}C-abundance. The clustering analysis was carried out with the Cluster software and the array is drawn using the TreeView software (both are from M. Eisen, Standford University).

Acknowledgements. We thank the Institut Fédératif de Recherche 87 for its support through a Transversal Project grant. Dr G. Tcherkez wishes to thank Dr. Jean Vidal for valuable discussions on the manuscript.

References

1 Krebs, H. A. & Johnson, W. A. (1937) Biochem. J. 31, 645-660.
2 Krebs, H. A. & Johnson, W. A. (1937) Enzymologia 4, 148-156.
3 Nunes-Nesi, A., Sweetlove, L. J. & Fernie, A. R. (2007) Physiol. Plant. 129, 45-56.
4 Atkin, O. K., Millar, A. H., Gärdestrom, P. & Day, D. A. (2000) in Photosynthesis, Physiology and Metabolism, eds Leegood, R. C., Sharkey, T. D. & von Caemmerer, S. (Kluwer Academic Publisher, London), pp. 203-220.
5 Cornic, G. (1973) Physiol. Vég. 11, 663-679.
6 Budde, R. J. A. & Randall, D. D. (1990) Proc. Natl. Acad. Sci. USA 87, 673-676.
7 Tovar-Mendez, A., Miernyk, J. A. & Randall, D. D. (2003) Eur. J. Biochem. 270, 1043-1049.
8 Hanning, I. & Heldt, H. W. (1993) Plant Physiol. 103, 1147-1154.
9 Tcherkez, G., Cornic, G., Bligny, R., Gout, E. & Ghashghaie, J. (2005) Plant Physiol. 138, 1596-1606.
10 McCashin, B. G., Cossins, E. A. & Canvin, D. T. (1988) Plant Physiol. 87, 155-161.
11 Igamberdiev, A. U. & Gardeström, P. (2003) Biochim. Biophys. Acta 1606, 117-125.
12 Plaxton, W. C. (1996) Annu. Rev. Plant Physiol. Plant Mol. Biol. 47, 185-214.
13 Tcherkez, G. & Hodges, M. (2007) J. Exp. Bot., in press.
14 Pinelli, P. & Loreto, F. (2003) J. Exp. Bot. 54, 1761-1769.
15 Messinger, S. M., Buckley, T. N. & Mott, K. A. (2006) Plant Physiol. 140, 771-778.
16 Stitt, M. (1990) Annu. Rev. Plant Physiol. Plant Mol. Biol. 41, 153-185.
17 Huppe, H. C. & Turpin, D. H. (1994) Annu. Rev. Plant Mol. Biol. Plant Physiol. 45, 577-607.
18 Lin, M., Turpin, D. H. & Plaxton, W. C. (1989) Arch. Biochem. Biophys. 269, 228-238.
19 Gardeström, P. & Wigge, B. (1988) Plant Physiol. 88, 69-76.
20 Bykova, N. V., Keerberg, O., Pärnik, T., Bauwe, H. & Gardeström, P. (2005) Planta 222, 130-140.
21 Day, D. D., Neuburger, M. & Douce, R. (1985) Aust. J. Plant Physiol. 12, 119-130.
22 Irendale, S. E. (1979) Phytochemistry 18, 1057-1058.
23 Chen, R. D. & Gadal, P. (1990) Plant Physiol. Biochem. 28, 141-145.
24 Rachmilevitch, S., Cousins, A. B. & Bloom, A. J. (2004) Proc. Nat. Acad. Sci. USA 101, 11506-11510.
25 Bloom, A. J., Smart, D. R., Nguyen, D. T. & Searles, P. S. (2002) Proc. Nat. Acad. Sci. USA 99, 1730-1735.
26 Priault, P., Tcherkez, G., Cornic, G., DePaepe, R., Naik, R., Ghashghaie, J. & Streb, P. (2006) J. Exp. Bot. 57, 3195-3207.
27 Dutilleul, C., Lelarge, C., Prioul, J. L., DePaepe, R., Foyer, C. H. & Noctor, G. (2005) Plant Physiol. 139, 64-78.

28 Thomas, R. B., Reid, C. D., Ybema, R. & Strain, B. R. (1993) Plant Cell Environ. 16, 539-546.
29 Shapiro, J. B., Griffin, K. L., Lewis, J. D. & Tissue, D. T. (2004) New Phytol. 162, 377-386.
30 Tcherkez, G., Nogués, S., Bleton, J., Cornic, G., Badeck, F. & Ghashghaie, J. (2003) Plant Physiol. 131, 237-244.
31 Evans, J. R., Sharkey, T. D., Berry, J. A. & Farquhar, G. D. (1986) Aust. J. Plant Physiol. 13, 281-292.
32 Aubert, S., Gout, E., Bligny, R., Marty-Mazars, D., Barrieu, F., Alabouvette, J., Marty, F. & Douce, R. (1996) J. Cell Biol. 133, 1251-1263.
33 Gout, E., Bligny, R., Pascal, N. & Douce, R. (1993) J. Biol. Chem. 286, 3986-3992.
34 Nogués, S., Tcherkez, G., Cornic, G. & Ghashghaie, J. (2004) Plant Physiol. 136, 3245-3254.
35 Tcherkez, G., Ghashghaie, J. & Griffiths, H. (2007) Plant Cell Environ. 30, 887-891.

Figure 1. **A**, carbon isotope discrimination (Δ_{obs}) associated with photosynthesis of detached leaves (at 21°C and 400 μmol m^{-2} s^{-1} PPFD) fed with either ^{13}C-1- or ^{13}C-2-enriched Pyr under four CO_2/O_2 conditions: 140, 400 or 1000 μL L^{-1} CO_2 in 21% O_2, and 400 μL L^{-1} CO_2 in 2% O_2. **B**, carbon isotope composition ($\delta^{13}C$) of respired CO_2 in darkness after the corresponding light periods. When leaves experienced a light period under 2% O_2, the carbon isotope composition was measured in either 21% (indicated as '400 μL L^{-1}, 2-21%') or 2% O_2 (indicated as '400 μL L^{-1}, 2-2%'). Each value is the mean±SE of three measurements. The control $\delta^{13}C$ value of respired CO_2 was –22.1±0.5‰.

Figure 2. Decarboxylation rates and inhibition of decarboxylation by light calculated from data of Fig. 1, using the method of ref. (9). The decarboxylation rates by PDH (white bars) and the TCA cycle (black bars) are given in the light (panel **A**, denoted as r_{light} just below) and in the dark (panel **B**, denoted as r_{night} just below). Inhibition by light (calculated as 1 – r_{light}/r_{night}, in %) is indicated on panel **C**. Conditions experienced by leaves during the light period are indicated on the *x* axis as in Fig. 1: 140, 400 and 1000 μL L^{-1} CO_2 in 21% O_2 and 400 μL L^{-1} CO_2 in 2% O_2. The $\delta^{13}C$ values of dark-respired CO_2 obtained in 2% O_2 (Fig. 1B right bars) were used to calculate the inhibition value after a light period in 2% O_2.

Figure 3. Isotopomics array representation of ^{13}C-abundance in the carbon atom positions of major metabolites in detached leaves incubated with ^{13}C-substrates for 2 h at 21°C, 21% O_2 and 400 μmol m^{-2} s^{-1} PPFD. CO_2 mole fraction was 140 μL L^{-1}, 400 μL L^{-1}, and 1000 μL L^{-1}. At t = 2 h, leaves were immediately frozen in liquid nitrogen for perchloric acid extraction. Perchloric extracts were analysed for positional ^{13}C-abundances by NMR. Each column is a separate set of experimental conditions. Cit, citrate; Fum, fumarate; Ido/Gal, uncertain D-hexofuranose belonging to the idose-galactose group; Mal, malate; Obt, oxobutyrate; SF and

SG, fructosyl and glucosyl moieties of sucrose, respectively. Red and green cells indicate ^{13}C-abundances above and below the natural abundance (which is 1.1%). Below-natural abundance cells appear dark-green because the ^{13}C-abundance is still very close to 1.1%.

Figure 4. **Main panel.** ^{13}C-abundance in glutamate (Glu, black bars), succinate (Succ, light-grey bars) and fumarate (Fum, dark-grey bars), relative to that in malate. Values are from the data of Fig. 3. The three different CO_2 mole fractions (in μmol mol^{-1}) used in the experiment are indicated on the *x* axis. **Inset.** Data of Fig. 3, replotted to show the relationship between the positional ^{13}C-abundance (in % of ^{13}C) in malate C-2 (triangles), fumarate C-2/3 (circles) and glutamate C-2 (squares) and the quantity of metabolite (in μmol per gram of fresh weight). Short dashed lines indicate exponential decay (fumarate and malate) and linear (Glu) regressions; both are significant: F=7.26 (P<0.005) and F=16.38 (P<0.003), respectively.

Figure 5. Relationship between the inhibition of the TCA cycle in the light (in %, data from Fig. 2) and the dihydroxyacetone phosphate (DHAP) to inorganic phosphate (Pi) (open discs) or Glc-6-phosphate (closed disks) ratio. Phosphorylated compounds were measured by ^{31}P-NMR on the same samples used for ^{13}C-NMR after ^{13}C-labeling. Lines stand for linear regressions. The regression with DHAP/Glc-6-P is significant (F=61.7, P<0.08).

Figure 1

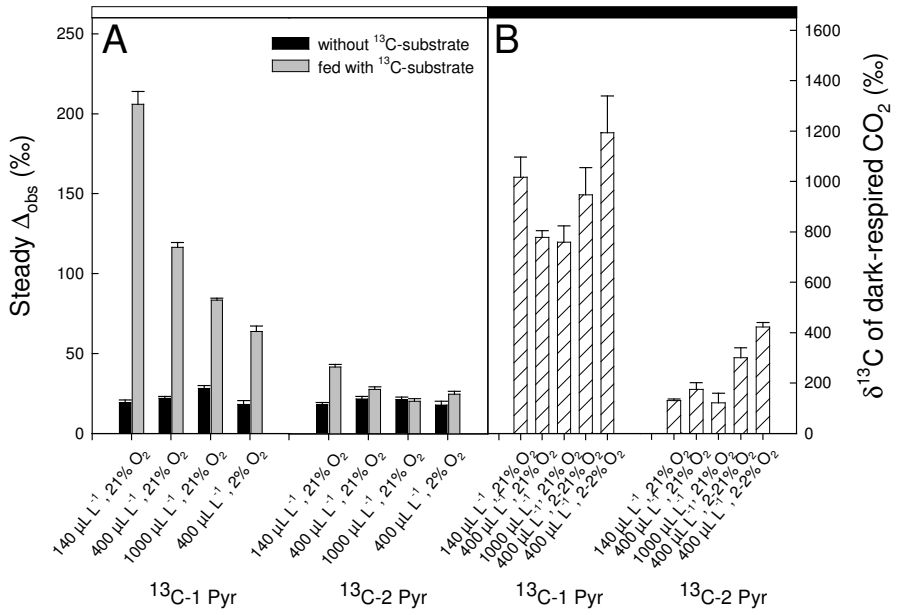
A
B
without ^{13}C-substrate
fed with ^{13}C-substrate
Steady Δ_{obs} (‰)
δ^{13}C of dark-respired CO_2 (‰)
0
50
100
150
200
250
0
200
400
600
800
1000
1200
1400
1600
140 µL L^{-1}, 21% O_2
400 µL L^{-1}, 21% O_2
1000 µL L^{-1}, 21% O_2
400 µL L^{-1}, 2% O_2
^{13}C-1 Pyr
^{13}C-2 Pyr

Figure 2

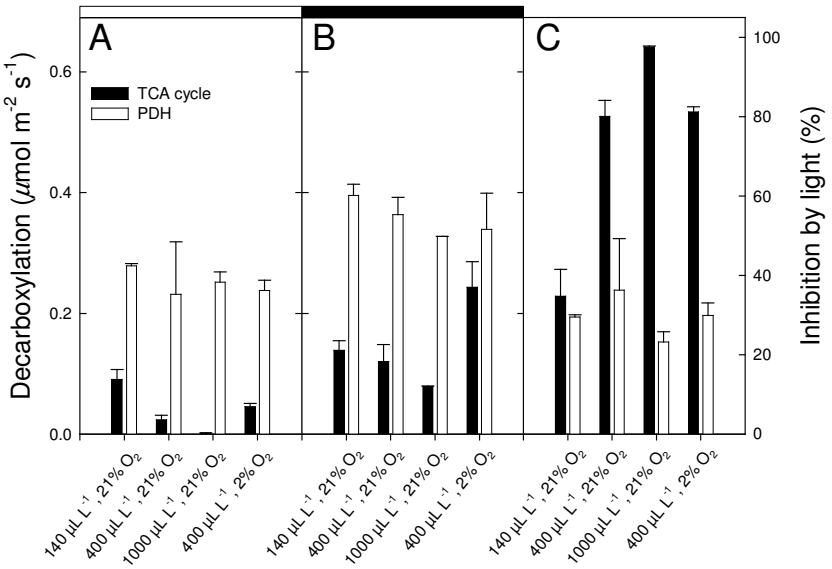
A
B
C
TCA cycle
PDH
Decarboxylation (μmol m-2 s-1)
Inhibition by light (%)
0.0
0.2
0.4
0.6
0
20
40
60
80
100
140 μL L-1, 21% O2
400 μL L-1, 21% O2
1000 μL L-1, 21% O2
400 μL L-1, 2% O2

Figure 3

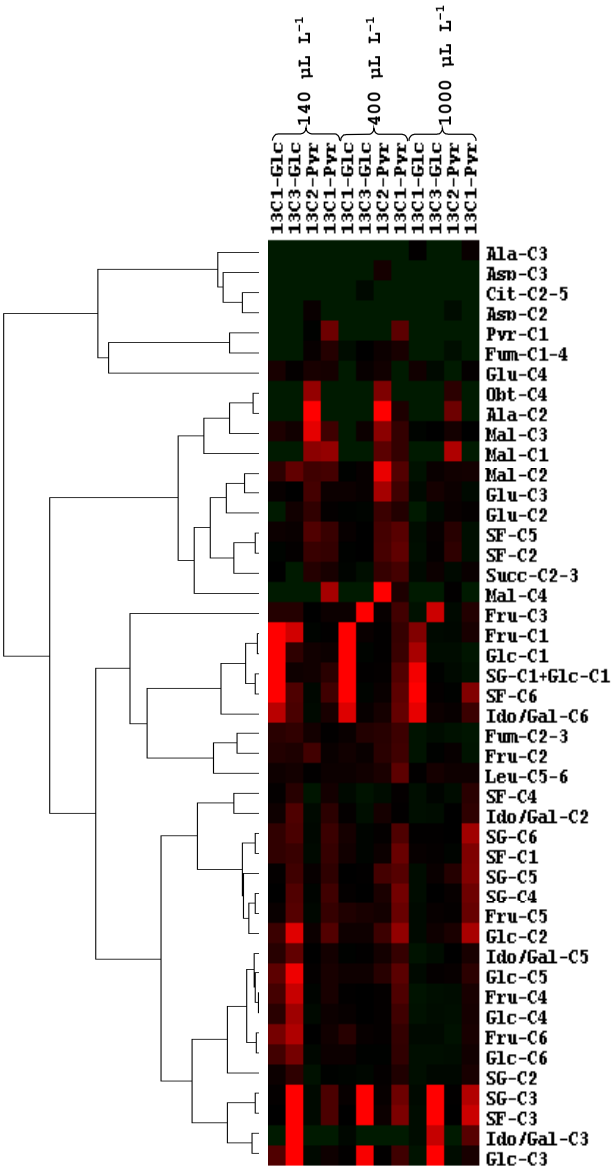
140 µL L-1
400 µL L-1
1000 µL L-1
13C1-Glc
13C3-Glc
13C2-Pyr
13C1-Pyr
13C1-Glc
13C3-Glc
13C2-Pyr
13C1-Glc
13C3-Glc
13C2-Pyr
13C1-Pyr
Ala-C3
Asn-C3
Cit-C2-5
Asn-C2
Pyr-C1
Fum-C1-4
Glu-C4
Obt-C4
Ala-C2
Mal-C3
Mal-C1
Mal-C2
Glu-C3
Glu-C2
SF-C5
SF-C2
Succ-C2-3
Mal-C4
Fru-C3
Fru-C1
Glc-C1
SG-C1+Glc-C1
SF-C6
Ido/Gal-C6
Fum-C2-3
Fru-C2
Leu-C5-6
SF-C4
Ido/Gal-C2
SG-C6
SF-C1
SG-C5
SG-C4
Fru-C5
Glc-C2
Ido/Gal-C5
Glc-C5
Fru-C4
Glc-C4
Fru-C6
Glc-C6
SG-C2
SG-C3
SF-C3
Ido/Gal-C3
Glc-C3

Figure 4

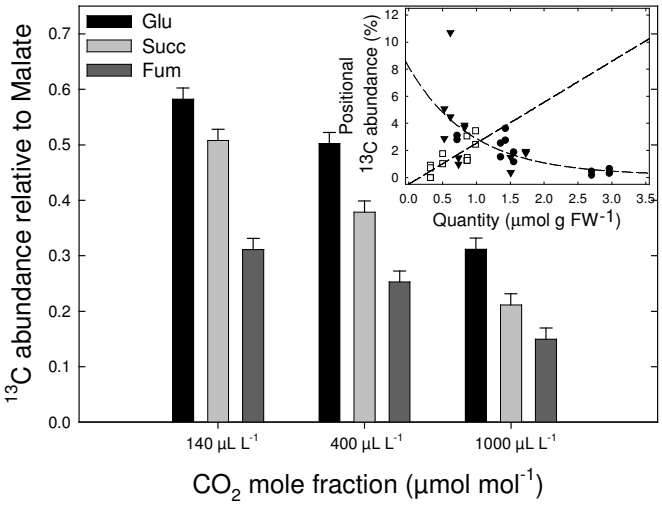
Glu
Succ
Fum
^{13}C abundance relative to Malate
0.0
0.1
0.2
0.3
0.4
0.5
0.6
0.7
140 µL L^{-1}
400 µL L^{-1}
1000 µL L^{-1}
CO$_2$ mole fraction (µmol mol^{-1})
Positional ^{13}C abundance (%)
0
2
4
6
8
10
12
0.0 0.5 1.0 1.5 2.0 2.5 3.0 3.5
Quantity (µmol g FW^{-1})

Figure 5

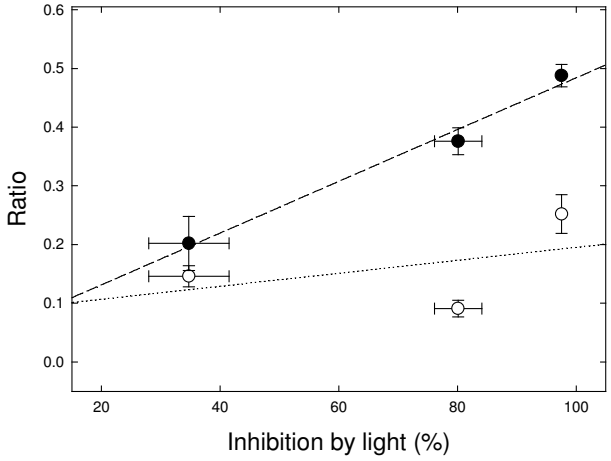

Supporting information (for on-line publication)

Table S1. Apparent photosynthetic carbon isotope discrimination (Δ_{obs}) and carbon isotope composition of dark-respired CO_2 ($\delta^{13}C$) of detached leaves fed with ^{13}C-1- or ^{13}C-3-Glc. Conditions during the light period are 140 and 400 µL L^{-1} CO_2 in 21% O_2 under 400 µmol m^{-2} s^{-1} PPFD. In water (no feeding conditions), the Δ_{obs} value is 21.6±1.2‰. The $\delta^{13}C$ value of respired CO_2 in darkness in water (no feeding) is -34.5±0.8‰ and -42.0±0.7‰ after a light period under 140 µL L^{-1} and 400 µL L^{-1} CO_2, respectively. Mean and SE of three measurements.

140 µL L^{-1} CO_2 in 21% O_2				400 µL L^{-1} CO_2 in 21% O_2			
^{13}C-1-Glc		^{13}C-3-Glc		^{13}C-1-Glc		^{13}C-3-Glc	
Light	Darkness	Light	Darkness	Light	Darkness	Light	Darkness
Δ_{obs}, ‰	$\delta^{13}C$, ‰	Δ_{obs}, ‰	$\delta^{13}C$, ‰	Δ_{obs}, ‰	$\delta^{13}C$, ‰	Δ_{obs}, ‰	$\delta^{13}C$, ‰
56.0±5.6	386±8	106.4±13.8	719±30	23.8±1.0	245±8	23.8±1.0	365±33

Table S2. Glucose decarboxylation rates and inhibition of decarboxylation by light, using the method of ref. (9) and data from Table S1. The decarboxylation rates by PDH and the TCA cycle are given in the light (denoted as r_{light} just below) and in the dark (denoted as r_{night} just below). Inhibition by light (calculated as $1 - r_{light}/r_{night}$, in %) is indicated on the right.

	140 µL L^{-1} CO_2 in 21% O_2		400 µL L^{-1} CO_2 in 21% O_2	
	PDH decarboxylation	TCA decarboxylation	PDH decarboxylation	TCA decarboxylation
Decarboxylation value in the light, µmol m^{-2} s^{-1}	0.067±0.011	0.111±0.001	0.007±0.001	0.019±0.001
Decarboxylation value in darkness, µmol m^{-2} s^{-1}	0.205±0.017	0.267±0.001	0.074±0.001	0.204±0.001
Inhibition by light, %	67.4±2.8	58.5±0.1	89.4±0.7	90.7±0.1

Table S3. Carbon isotope composition of starch (in ‰) after feeding leaves with ^{13}C-enriched Glc (δ^{13}C=2500‰) or Pyr (δ^{13}C=1400‰) in the light under different CO_2/O_2 conditions (experiment described in Figure 1) and associated contributions of ^{13}C-enriched substrates to starch synthesis. The δ^{13}C value of CO_2 used in the open system is −50.2‰. Samples were immediately frozen in liquid nitrogen after 2 hours feeding, for starch extraction. The contribution values assume refixation of the ^{13}C-enriched decarboxylated CO_2 and do not take into account the global δ^{13}C of added substrate. Contributions given in µmol m^{-2} s^{-1} are average values over the 2 h feeding period. Mean and SD of three measurements.

	140 µL L^{-1} CO_2 in 21% O_2				400 µL L^{-1} CO_2 in 21% O_2				1000 µmol mol^{-1} CO_2 in 21% O_2		400 µmol mol^{-1} CO_2 in 2% O_2	
	^{13}C-1-Pyr	^{13}C-2-Pyr	^{13}C-1-Glc	^{13}C-3-Glc	^{13}C-1-Pyr	^{13}C-2-Pyr	^{13}C-1-Glc	^{13}C-3-Glc	^{13}C-1-Pyr	^{13}C-2-Pyr	^{13}C-1-Pyr	^{13}C-2-Pyr
No feeding	–28.0±1.0				–31.4±0.4				–35.4±0.9		–33.0±0.9	
Fed leaf	-12.7±0.5	-27.4±0.4	-18.3±0.5	-13.3±0.6	-21.8±1.0	-29.9±0.7	-27.3±0.6	-27.7±0.2	-36.5±0.5	-32.5±0.4	-22.3±0.3	-27.4±0.7
Contribution (%)	0.37	0.01	0.13	0.20	0.23	0.03	0.06	0.05	0	0.06	0.26	0.13
Contribution (µmol m^{-2} s^{-1})	0.06	0	0.02	0.03	0.04	0.01	0.01	0.01	0	0.01	0.04	0.02